Heliyon 9 (2023) e16979

Contents lists available at ScienceDirect

Heliyon

journal homepage: www.cell.com/heliyon

Effect of Co-existing gases on hydrogen permeation through a Pd82–Ag18/α-Al_2O_3 membrane during transient start-up

Yogi Wibisono Budhi [a,b,c,*], Hans Kristian Irawan [a], Raihan Annisa Fitri [a], Tareqh Al Syifa Elgi Wibisono [a], Elvi Restiawaty [c,d], Manabu Miyamoto [e], Shigeyuki Uemiya [e]

[a] *Department of Chemical Engineering, Faculty of Industrial Technology, Institut Teknologi Bandung, Jl. Ganesha 10, Bandung 40132, Indonesia*
[b] *Research Center for Nanosciences and Nanotechnology, Institut Teknologi Bandung, Jl. Ganesha 10, Bandung 40132, Indonesia*
[c] *Research Group of Chemical Engineering Process Design and Development, Faculty of Industrial Technology, Institut Teknologi Bandung, Jl. Ganesha 10, Bandung 40132, Indonesia*
[d] *Department of Bioenergy Engineering and Chemurgy, Faculty of Industrial Technology, Institut Teknologi Bandung, Jl. Let. Jend. Purn. Dr. (HC) Mashudi No.1, West Java 45363, Indonesia*
[e] *Department of Chemistry and Biomolecular Science, Faculty of Engineering, Gifu University, 1-1 Yanagido, Gifu 501-1193, Japan*

A R T I C L E I N F O

Keywords:
Pd-Ag membrane
Gas separation
Hydrogen recovery
Counter-current
Sieverts-Fick

A B S T R A C T

The work aimed to study the influence of co-existing gaseous mixture (H_2–N_2–CO–CO_2) on hydrogen permeation through the counter-current flow of a Pd82–Ag18/α-Al_2O_3 membrane during transient start-up at 350 °C and atmospheric pressure. The membrane was operated for an 8-h. Its performance was measured in terms of hydrogen flux and recovery. The results were mapped on Sieverts-Fick's line and showed a slight membrane deactivation because of the presence of N_2 and CO_2 in the feed gas. The membrane deactivation became more profound when CO was a constituent. The effect of the co-existing gases on the hydrogen flux, in increasing order, was CO > CO_2>N_2. The co-existing gases, if present as a significant fraction, induces dilution, concentration polarization, and inhibition over the membrane surface, decreases the membrane performance in term of hydrogen recovery, time lag during transient start-up, and deactivation. It is recommended that the start-up might be run using equimolar H_2–N_2 mixture.

1. Introduction

Hydrogen has the advantages of being a viable future energy carrier, including environmental friendliness, high electrical energy conversion efficiency, and high energy density. Hydrogen is classified as green, grey, or blue depending on how it is produced. Green hydrogen, which is primarily produced through electrolysis, is carbon-neutral hydrogen because no carbon is produced during the production process or consumption as a fuel. Grey hydrogen is produced by reforming process from natural gas, coal, and heavy oil. When the carbon produced during extraction or manufacturing is captured and stored, grey hydrogen is improved to blue hydrogen [1]. Hydrogen separation and purification processes are categorized as membrane separation [2,3], pressure swing adsorption [4,5], low-temperature separation [6], metal hydride method [7,8], and catalytic deoxygenation [9]. Separation technology with membrane

* Corresponding author. Department of Chemical Engineering, Faculty of Industrial Technology, Institut Teknologi Bandung, Jl. Ganesha 10, Bandung 40132, Indonesia.

E-mail address: Y.Wibisono@itb.ac.id (Y.W. Budhi).

https://doi.org/10.1016/j.heliyon.2023.e16979
Received 22 April 2023; Received in revised form 9 May 2023; Accepted 2 June 2023
Available online 3 June 2023

has advantages in improving efficiency, reducing capital and operational costs, increasing hydrogen yield and selectivity, and reducing CO_2 emissions. Pd-based membranes exhibit good permeability (Pe_{H_2}) and selectivity to hydrogen [10–14]. Pd membranes are usually combined with other metals, such as silver and/or ceramic buffers, such as alumina [15–20]. Due to the high permeability of Pd and its alloys (Ag, Cu, Au) for hydrogen, palladium-based membranes have the ability to extract high flux with high perm selectivity among all H_2-selective membranes [21] to increase their mechanical strength. Various variables affect the hydrogen permeation through the Pd membrane, including the influence of pressure and temperature on H_2 production [19]. Furthermore, Faizal et al. [20] studied the effect of feed gas flow rate on hydrogen permeation. Barreiro et al. [10] observed the influence of temperature, pressure, flow rate, and feed gas concentration on Pe_{H_2}. The effects of CO, CO_2 and H_2O on H_2 permeation were reported by Hou and Houghes [22], Boon et al. [23], Sakamoto et al. [24], and Goldbach et al. [25]. N_2 gas inhibits H_2 permeation through the Pd–Ag membrane by forming NH_x on the membrane surface [26] and can be regenerated at a temperature of >773 K by flushing using pure H_2. However, due to dilution, concentration polarization, and competitive adsorption, H_2 production becomes discontinuous when flushing, and NH_x compounds reduce the H_2 permeation flux through the Pd membrane wall. The partial pressure of H_2 in feed gases containing H_2 and other gases is also lower than that of pure H_2 [27,28]. This is the leading cause of reduced H_2 permeation, which results in a smaller H_2 permeation flux. Compounds other than H_2 can also cause concentration polarization [29]. Gases that cannot penetrate the membrane create a concentration gradient above the surface of the membrane, blocking the H_2 permeation. This phenomenon is known as the "external mass-transfer resistance" of the membrane as studied by Budhi et al. [30–32] on a 100 μm Pd75–Ag25 membrane without support. Hou and Hughes [22] examined the influence of CO, CO_2, and H_2O on the Pd–Ag membrane. The inhibitory effect follows the $H_2O > CO > CO_2$ sequence, which correlates with the adsorption ability of this compound on the surface of the membrane. These gases create a significant inhibitory effect as their concentration increases, but their impact decreases at temperatures above 400 °C. The influence of CO_2 is insignificant at temperatures above 325 °C. Some other researchers [also observed a similar phenomenon, and a decrease in the H_2 flux occurred only due to the concentration of polarization [36]. Barbieri et al. [37] reported that CO_2 and N_2 were insignificant in inhibiting Pd–Ag membranes at 374 °C and 100 kPa. A mixture of H_2 with CO_2 and/or N_2 is still on the Sieverts-Fick line, showing a decrease in H_2 flux due to dilution. Israni et al. [38,39] found significant CO_2 inhibition at temperatures below 300 °C, while Gallucci et al. [40] results were similar to Barbieri et al. [37]. Barbieri et al. [37] proposed the joint law of Sievert and Langmuir isotherms to estimate H2 flux with CO. Li et al. Scura et al., Mejdell et al. Caravella et al., and Kurokawa et al. [27,37,41–43] reported a significant reduction in H_2 permeation at low temperatures. It is minimized if the operating temperature is ≥ 477 °C after evaluating the effect of temperature and CO on the feed gas. Scura et al. [37] reported reversible CO inhibitory effects, and the influence of other compounds was summarized by Unemoto et al. [44]. Li et al. [41] reported CO inhibition on the Pd membrane reduced H_2 permeation as the duration of the operation increased. Israni et al. [38] reported that the thin membrane of Pd–Ag was developed by stacking it on α-Al2O3 as a support, which increases the possibility of engineering application at high pressures. Adding Ag increases H_2 permeation and reduces the effect of NH_x inhibition on the membrane. The Pd–Ag membrane and α-Al_2O_3 buffer combination is expected to provide better H_2 separation performance than a pure Pd membrane. The performance of the membrane can be quantified through Pe_{H_2}. The performance reliability of membrane work is also affected by the dynamics of hydrogen permeability and mechanical properties caused by structural and superficial changes at membrane work in gaseous media [45]. Thus, this study is focused on observing the effects of co-existing gases, such as H_2, N_2, CO, and CO_2, on the permeation of H_2 through a Pd82–Ag18/α-Al_2O_3membrane. Observations were made on a mixture of H_2 gas with N_2, CO, and CO_2 in binary, ternary, or quaternary gaseous mixtures. The membrane stability of Pd82–Ag18/α-Al_2O_3 as a function of time was assessed during a start-up operation of approximately 8 h at a temperature of 350 °C.

2. Experiments

An experimental setup was designed provide the laboratory work to run the Pd82–Ag18/α-Al_2O_3 membrane for H_2 separation. In each experiment, the feed gas was made to flow to the membrane on the feed side, while the sweep gas (N_2) was made to continuously flow at a rate of 120 mL/min on the permeate side. The feed and sweep gases were fed in a counter-current flow configuration, based on a study by Caravella et al. [46]. After the equipment was assembled, a leak test was performed for each hose connection by applying soap on the same and checking if bubbles were released from the connection. The H_2 compositions in the feed and retentate streams were measured using a gas detector (Cosmos XP-3140, New Cosmos Electric Co., Ltd., Japan). In this case, N_2 should not penetrate through the membrane wall, and thus the permeate side output should be pure H_2. In addition, before the membrane system was used, it was cleaned by purging by the use of ultra-high-pure argon for approximately 30 min. This would eliminate any non-inert gases on the membrane surface. During this time, the membrane was heated up to a desired operating temperature (350 °C). For the following 30 min, ultra-high-pure- H_2 and argon were simultaneously introduced into the membrane to remove all adsorbed compounds over the membrane surface. With this activation stage, the initial state of the membrane would always be clean and in the same condition. In the next 30 min, only argon was fed into the module to ensure that the membrane was free of H_2.

2.1. Hydrogen separation

The main experiments were carried out with a mixed gas flow of H_2, N_2, CO, and CO_2. In each experiment, the sweep gas of N_2 was continuously made to flow at a rate of 120 mL/min on the permeate side to create a partial pressure difference between the retentate and permeate sides. The concentration of the permeate gas was measured by the H_2 gas online sampling system (Cosmos XP-3140, thermal conductivity). The membrane performance was expressed in terms of the hydrogen recovery and the hydrogen flux.

2.2. Data interpretation

The hydrogen recovery was determined from the H_2 composition taken from the flow rate measurement. The data were treated, and a reproducibility test was also performed.

2.2.1. Permeability of Pd membrane

The Pe_{H_2} of the Pd82–Ag18/α-Al_2O_3 membrane was calculated using the following equations:

$$I_{H2} = \frac{Pe_{H2}}{\delta}\left[\left(P_{H2}^{shell}\right)^{0.5} - \left(P_{H2}^{tube}\right)^{0.5}\right] \quad (1)$$

$$P_{H2}^{0.5} shell = \left(y_{H2,shell}\,P_{atm}\right)^{0.5} \quad (2)$$

$$P_{H2}^{0.5} tube = \left(y_{H2,tube}\,P_{atm}\right)^{0.5} \quad (3)$$

where J_{H_2} = molar flux of hydrogen $(\text{mol m}^{-2}\ \text{s}^{-1})$, Pe_{H_2} = permeability value of membrane $(\text{mol m}^{-1}\ \text{s}^{-1}\ \text{Pa}^{-0.5})$, δ = membrane thickness (m), $P_{H_2,\text{tube}}$ = partial pressure of H_2 on permeate side (Pa), $P_{H_2,\text{shell}}$ = partial pressure of H_2 on feed side (Pa), $y_{H_2,\text{tube}}$ = mole fraction of hydrogen on permeate side, and $y_{H_2,\text{shell}}$ = mole fraction of hydrogen on feed side.

2.2.2. Determination of hydrogen recovery

The determination of hydrogen recovery (*HR*) of the Pd82–Ag18/α-Al_2O_3 membrane was conducted by comparing the H_2 flow rate on the permeate side to the total flow rate of H_2 in the feed. *HR* can be calculated using Equation (4).

$$HR = \frac{F_{permeat} \bullet x_{H2permeat}}{F_{membrane\ feed} \bullet x_{H2membranefeed}} \quad (4)$$

2.3. Pd82–Ag18/α-Al_2O_3 membrane

The Pd82–Ag18/α-Al_2O_3 membrane used in this study was synthesized by electroless plating over the outer surface of a porous α-Al_2O_3 tube [32,47,48]. The technical specifications are as follows: outer and inner diameters are 10 and 7 mm, respectively; membrane thickness of 20.2 μm; membrane length of 80 mm; and a mean pore diameter of the support of 0.1 μm [49]. Its cross-over surface was analyzed by scanning electron microscope (SEM). In addition, an energy dispersive X-Ray (EDX) analysis was conducted to investigate the distribution of Ag in the Pd82–Ag18/α-Al_2O_3 membrane. The characterization results are presented in Fig. 1. Based on the SEM analysis, no pinholes were observed. This indicates that the Pd82–Ag18/α-Al_2O_3 membrane has been prepared in a good condition. Furthermore, from the images obtained through the EDX analysis, it could be seen that the distribution of Ag was uniform at an average of 18.2 wt%.

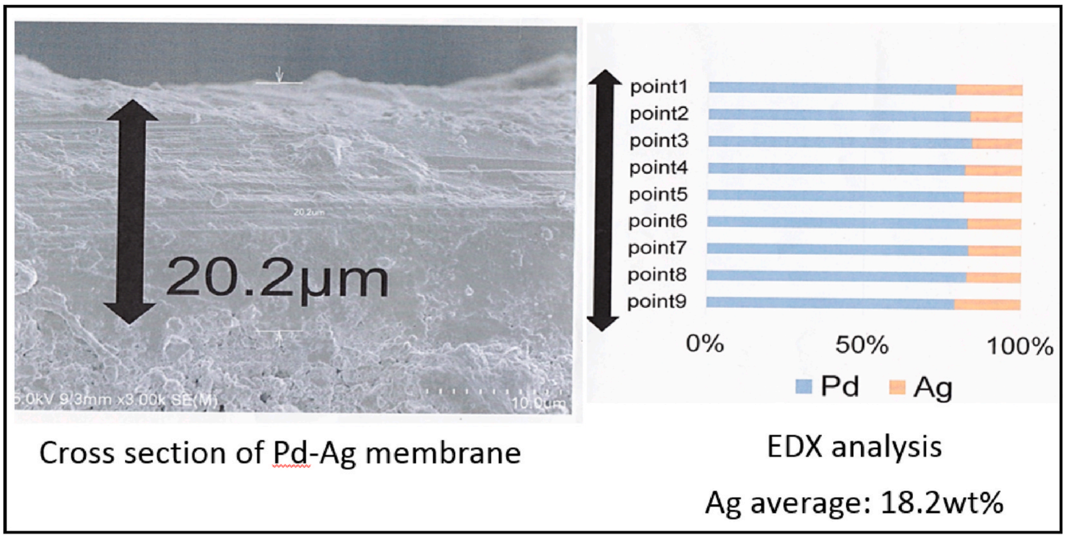

Fig. 1. SEM image and EDX analysis over Pd82–Ag18/α-Al_2O_3 membrane.

2.4. Variation of experiments

The experimental runs performed in this study are summarized in Table 1 for binary compositions of H_2–N_2 (run 1–3), H_2–CO_2 (run 4–5), H_2–CO (run 7), for ternary compositions of H_2–N_2–CO_2 (run 6), H_2–CO_2–CO (run 8), and H_2–N_2–CO (run 9). Experimental variations were selected based on the typical output of a secondary reformer in an ammonia plant, which followed a composition consisting of 56%-mole H_2; 24%-mole N_2; and 14%-mole CO; with the balance being CO_2 (run 10). The reproducibility test was accomplished by taking sample for Run 2 (named Run 11). The influence of temperature was only investigated in experiments involving H_2 and CO (Run 12).

3. Results and discussion

3.1. Determination of hydrogen permeability of the Pd82–Ag18/α-Al_2O_3 membrane

The effect of H_2 partial pressure on the retentate and permeate sides of the Pd-based membrane plays an important role in the separation of H_2. This is in line with Sieverts-Fick's law, which states that the higher the partial pressure difference between the retentate and permeate sides, the greater the driving force on H_2 to permeate. This principle can be used to determine the membrane's Pe_{H_2} constant. In this study, the determination of the membrane's Pe_{H_2} constant was carried out by passing pure H_2 feed at a flow rate of 90 mL/min on the retentate side of the Pd82–Ag18/α-Al_2O_3 membrane, which was operated at a constant temperature of 350 °C. On the permeate side, a sweep gas of pure N_2 was introduced with a varying flow rate of 41 to 237 mL/min, thus leading to different levels of H_2 permeation. By plotting the H_2 flux as a function of the difference in the partial pressures between the retentate and permeate sides, the membrane's Pe_{H_2} constant could be determined (Equation (1)). The power value (n) in the partial pressure difference equation was set to 0.5 because the membranes used in the experiment were relatively thick (>10 μm) and operated at a low pressure. According to Basile et al. [50], when the membrane had a thickness >10 μm, and was operated at a sufficiently low pressure, the diffusion acted as a rate determinant; hence, the value of n was set to 0.5. This was confirmed by Caravella et al. [46], who reported the Pe_{H_2} on a Pd membrane with a thickness of 10 μm, at an operating temperature of 350 °C. They also found that under these conditions, the greatest resistance to H_2 permeation was offered by the diffusion of H_2 across the membrane. A plot of the hydrogen flux (J_{H_2}) versus the partial pressure difference between the feed and permeate sides is shown in Fig. 2. When the H_2 partial pressure difference between the feed and permeate sides was high, the H_2 flux passing through the membrane was also high. The slope of the curve was 16, which represents the value of $\frac{Pe_{H_2}}{\delta}$. Thus, from the value of the membrane layer thickness (δ), which was 20.2 μm, the membrane's Pe_{H_2} could be evaluated. The Pe_{H_2} of the Pd82–Ag18/α-Al_2O_3 membrane in this experiment was obtained as $3.23 \times 10^{-4}\ \frac{mol.m}{m^2 \bullet h \bullet kpa^{0.5}}$. A comparison of the Pe_{H_2} values in this study with the results of other researchers is presented in Table 2.

$$\left(P_{H_2}^{shell}\right)^{0.5} - \left(P_{H_2}^{tube}\right)^{0.5} \left(\text{kPa}^{0.5}\right)$$

From Tables 2 and it is seen that Pe_{H_2} of the Pd82–Ag18/α-Al_2O_3 membrane in this work had a value that agreed reasonably with the Pe_{H_2} values of various palladium-based membranes, as reported by several other researchers. These values were all of the order of 10^{-4} mol • m/(m^2 • h• kPa$^{0.5}$). The value of Pe_{H_2} for a Pd93–Ni7 membrane was smaller than that of the Pd82–Ag18/α-Al_2O_3 membrane (this study) because the former was thicker and operated at a lower temperature [51]. The greater membrane thickness resulted in a larger internal mass transfer resistance of the membrane, thus rendering the H_2 permeation more difficult. The same factor also caused the Pd–Ag membrane with a 50-μm thickness to have a smaller value of Pe_{H_2} [53]. Furthermore, the operating temperature affected the kinetic energy of the hydrogen molecules moving across the membrane. The higher the temperature, the better the Pe_{H_2}. This was also responsible for the Pd80–Ag20/ceramic membrane investigated by Pizzi et al. [54] to have a larger Pe_{H_2} value. On the

Table 1
Experimental variation.

Run	Interaction type	Feed composition (%-mole)			
		H_2	N_2	CO_2	CO
1	Binary H_2–N_2	52%	48%	–	–
2	Binary H_2–N_2	70%	30%	–	–
3	Binary H_2–N_2	77%	23%	–	–
4	Binary H_2–CO_2	87%	–	13%	–
5	Binary H_2–CO_2	54%	–	46%	–
6	Ternary H_2–N_2–CO_2	60%	30%	10%	–
7	Binary H_2–CO	80%	–	–	20%
8	Ternary H_2–CO_2–CO	68%	–	13%	19%
9	Ternary H_2–N_2–CO	62%	23%	–	15%
10	Quaternary H_2–N_2–CO_2–CO	56%	24%	9%	14%
11	Binary H_2–N_2 [a]	70%	30%	–	–
12	Binary H_2–CO *	80%	–	–	20%

Note: * operating temperature: 250 °C; the other experiments at 350 °C.
[a] For reproducibility test.

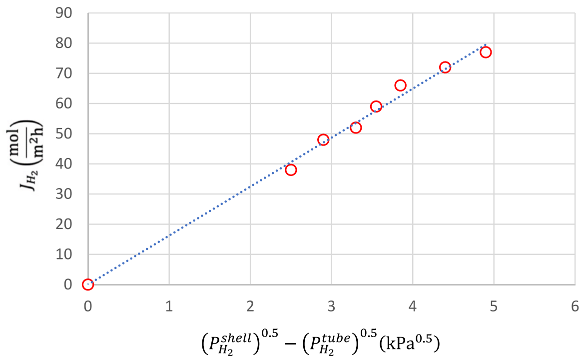

Fig. 2. Molar flux of hydrogen (J_{H_2}) as function of $[(P_{H_2}^{shell})^{0.5} - (P_{H_2}^{tube})^{0.5}]$.

Table 2
Comparison of permeability values Pe_{H_2} of various Pd based membranes.

Membrane Type	$Pe_{H_2}\ [\frac{mol.m}{m^2 \bullet h \bullet kpa^{0.5}}]$	δ [μm]	$T_{operating}$ [°C]	References
Pd93–Ni7	1.63×10^{-4}	100	300	Itoh and Xu [51]
Pd	1.59×10^{-4}	20	350	Chen and Chiu [52]
Pd–Ag	1.05×10^{-4}	50	350	Basile et al. [53]
Pd80–Ag20/ceramic	7.67×10^{-4}	2.5	400	Pizzi et al. [54]
Pd100/Al_2O_3	2.52×10^{-4}	20	350	Budhi et al. [32]
Pd82–Ag18/α-Al_2O_3	3.23×10^{-4}	20.2	350	This research

other hand, even though the membrane investigated by Budhi et al. [30]and the one employed in this work had identical membrane thicknesses, operating temperatures, and the same α-Al_2O_3 support, the Pd82–Ag18/α-Al_2O_3 membrane (of the current study) had a larger Pe_{H_2} than the Pd/α-Al_2O_3 membrane (used by Budhi et al. [32]). According to De Falco et al. [55], the addition of Ag on the Pd membrane could increase the Pe_{H_2} by up to 1.7 times. This was achieved by the addition of 23 wt% Ag. Consequently, when compared with the Pd/α-Al_2O_3 membrane, the Pe_{H_2} of the Pd82–Ag18/α-Al_2O_3 membrane was almost 1.3 times higher.

3.2. *Effect of N_2 on the performance of the Pd82–Ag18/α-Al_2O_3 membrane*

The effect of N_2 on the membrane performance was observed by passing a feed gas, consisting of a binary mixture of H_2/N_2, in which the fraction of N_2 was varied from 23% to 48% v/v. The experimental results of the stability of the Pd82–Ag18/α-Al_2O_3

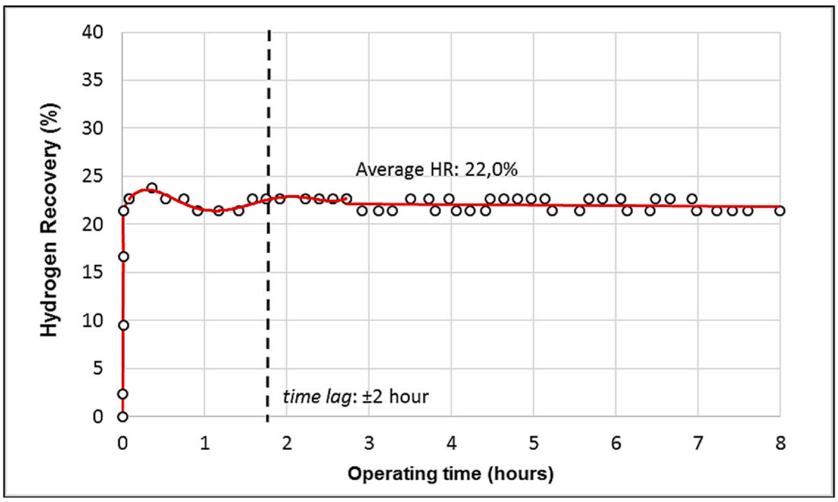

Fig. 3. The stability of hydrogen recovery (*HR*) throughout the membrane operation time of the feed gas which is a mixture of H_2/N_2 gas with a mole ratio of 52/48. White spots display *HR* per unit of experiment time; the red line is the auxiliary line to see the dynamic trend of *HR* every time; the black vertical dotted line represents the line indicating the time at which *HR* has stabilized. (For interpretation of the references to colour in this figure legend, the reader is referred to the Web version of this article.)

membrane under an 8-h operation, when H_2/N_2 was fed to the membrane with a composition 52% or 48% v/v, is shown in Fig. 3. Based on Fig. 3, the *HR* was calculated based on the ratio of the permeated H_2 and the amount of H_2 in the feed. An average *HR* value was calculated after the value stabilized. As observed, the *HR* fluctuated in the initial period of the membrane operation (start-up), and eventually became stable. The time required to a stable *HR* is called "time-lag," whose value was approximately 2 h. The *HR* fluctuated at the start-up because the hydrogen on the membrane surface underwent adsorption and desorption mechanisms to reach an equilibrium as finally indicated by steady state condition.

From the simulation results and experimental data, the J_{H_2} was obtained as 148.2 mol/(m^2·h). The counter-current operation resulted in approximately the same partial pressure difference between the two sides of the membrane at each particular position (approximately 41.4 kPa); therefore, the hydrogen flux along the membrane could be maintained under constant conditions. Thus, the reduction of H_2 flux along the membrane owing to depletion was not significant. The experimental results showing the effect of N_2 concentration variation on the membrane performance are summarized in Table 3. Fig. 4 shows the effect of the H_2 fraction in the feed on the H_2 flux.

The averaged *HR* (stable operation) was 22%. It was observed that there was no decrease in the hydrogen yield or membrane deactivation after the 8-h operation of the Pd82–Ag18/α-Al_2O_3 membrane, when a binary H_2/N_2 feed was introduced. Hou and Hughes [22] and Barbieri et al. [37] also reported similar results, which revealed that N_2 did not cause the deactivation of the Pd–Ag membrane. However, in a similar experiment using a Pd100/α-Al_2O_3 membrane, Budhi et al. [31] reported a decrease in the *HR* (due to membrane deactivation) during 8 h of operation. Thus, this current study confirmed the study of Chantaramolee et al. [12], which stated that the addition of Ag decreased the N atomic adsorption energy to the membrane and therefore, a deactivation due to N_2 did not occur.

From Table 3, we observe that the membrane operating lag time ranged from 2 to 3 h. At the start-up, the adsorption and desorption mechanisms moving towards an equilibrium were strongly influenced by the larger fraction of H_2 in the feed. In addition, from Table 3 and Fig. 4, it was found that the larger the H_2 fraction in the feed (or in other words the smaller the N_2 fraction), the greater the H_2 flux and *HR*. Peters et al. (2008) [47] and Caravella et al. (2010) [27] suggested that a decrease in the H_2 flux in multi-component feeds was caused by various factors, including dilution, and the presence of competitive adsorption or inhibition on the membrane surfaces. Fig. 4 shows the H_2 flux versus H_2 fraction of the feed to clarify the factors causing the decrease in the H_2 flux with increasing N_2 feed.

The hydrogen fraction in the feed was proportional to the partial pressure on the feed side. When the partial pressure on the permeate side was constant owing to the constant sweep gas rate, the slope of the graph between the H_2 fraction in the feed and H_2 flux was a fixed value, and followed Sieverts-Fick's law. From Fig. 4, it is seen that all the experimental points were in the region through which the Sieverts-Fick's line (red dashed line) passed. The existence of all the three test points on the line indicates that a decrease in the H_2 flux, when the amount of N_2 was increased was due to the dilution effect, and not the inhibition effect. This was also consistent with the results of the membrane stability experiment, which indicated the absence of membrane deactivation due to N_2 inhibition during the 8-h operation. This was in accordance with the results reported by Barbieri et al. [37].

3.3. *Effect of CO_2 on the performance of the Pd82–Ag18/α-Al_2O_3 membrane*

The effect of CO_2 on the membrane was observed by introducing a feed gas that was a binary mixture of H_2 and CO_2, in which the CO_2 fraction was varied between 13% and 46% (v/v). In addition, ternary feeds containing H_2, N_2, and CO_2 (60%, 30%, and 10% v/v, respectively) were also investigated. From the previous experiment, it was concluded that N_2 was inert on the surface of the membrane. One experimental result showing the Pd82–Ag18/α-Al_2O_3 membrane's stability for more than 7-h of operation, when fed with H_2 and CO_2 (87% and 13% v/v, respectively) is shown in Fig. 5.

Fig. 5 shows the *HR* over time for more than 7-h of membrane operation. The *HR* was calculated based on the ratio of the permeated H_2 to the amount of H_2 in the feed. The average *HR* score was calculated after the value became stable. In Fig. 5 it appears that the *HR* fluctuated during the start-up period, and eventually became stable. The fluctuations during the start-up period were more oscillatory than those in the experiments involving only H_2 and N_2. The time until the *HR* stabilization was attained was approximately 3 h. The *HR* fluctuated at start-up because the H_2 on the surface of the membrane underwent adsorption and desorption until equilibrium was reached [30]. The average *HR*, after the operation was stabilized, was approximately 36.4%. The CO_2 gas feed did not result in a significant deactivation of the Pd82–Ag18/α-Al_2O_3 membrane for more than 7 h. Some researchers found no significant effect of CO_2 on the membrane deactivation above 325 °C [10,22,23,36,40]. In addition CO_2 and N_2 did not cause significant inhibition of Pd–Ag membranes, when operated at 374 °C and 100 kPa [37].

The experimental results of the effect of CO_2 concentration variation on the membrane performance are summarized in Table 4,

Table 3
The comparison result of the performance Pd82–Ag18/α-Al_2O_3 membrane in the variation of binary H_2/N_2 feed.

	Run 1	Run 2	Run 3
H_2 fraction on feed	52%	70%	77%
N_2 fraction on feed	48%	30%	23%
Time lag (h)	±2.0	±2.8	±3.0
Partial pressure difference in each point of membrane length (kPa)	41.4	50.1	52.5
HR average (%)	22.0	29.2	33.1
$J_{H2[mole/(m^2\bullet h)]}$	148.2	220.5	248.8

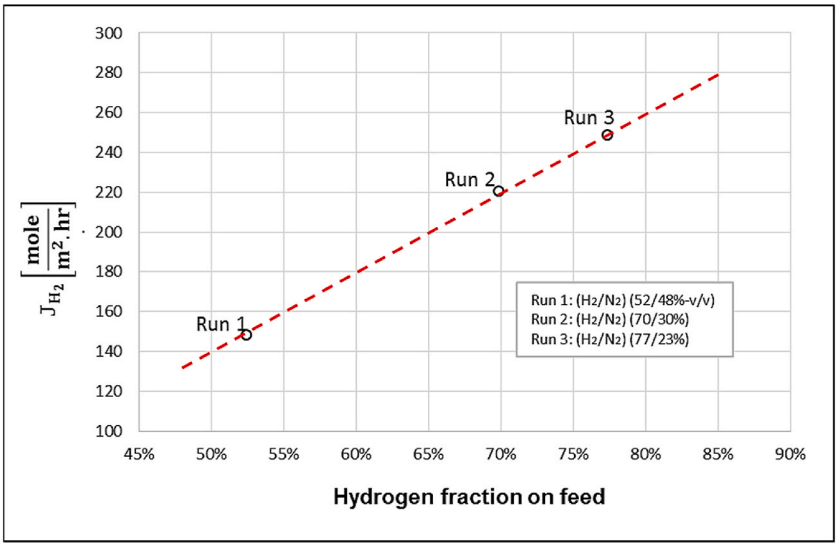

Fig. 4. Hydrogen fraction in feed to hydrogen flux due to N_2 gas. The red dotted line is the Sieverts-Fick's line. (For interpretation of the references to colour in this figure legend, the reader is referred to the Web version of this article.)

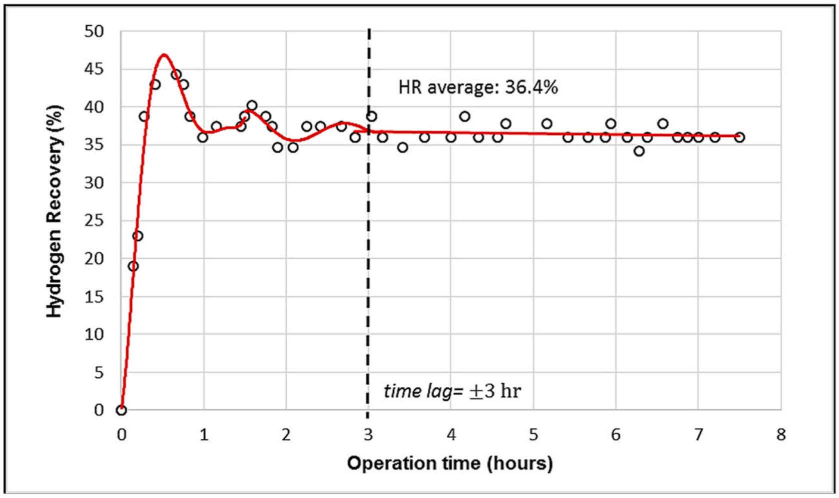

Fig. 5. The stability of hydrogen (HR) when binary feed gas of H_2/CO_2 with a mole ratio of 87/13 is introduced to membrane. White spots display HR on each observation time; the red line is the auxiliary line to see the dynamic trend of HR every time; the black vertical dotted line represents the line indicating the time at which HR has stabilized. (For interpretation of the references to colour in this figure legend, the reader is referred to the Web version of this article.)

Table 4
Result of observation of CO_2 effect on Pd82Ag18/α-Al_2O_3 membrane performance.

	Run 4	Run 5	Run 6
H_2 fraction on feed	87%	54%	60%
CO_2 fraction on feed	13%	46%	10%
N_2 fraction on feed	–	–	30%
Time lag (h)	±2.0	±3.0	±2.6
Pressure different on each relative position (kPa)	55.9	42.8	45.5
Averaged *HR* during stable oscillations period (%)	36.4	22.2	24.6
J_{H2} (mole/(m^2·h))	277.1	151.5	175.3

from which, it can be seen that the membrane operating lag time ranged from 2 to 3 h. It was also found that a larger H_2 fraction in the feed led to greater *HR* and H_2 flux (J_{H2}). Peters et al. [56] and Caravella et al. [27] suggested that the decrease in the H_2 flux in multi-component feeds was caused by various factors, including dilution, and the presence of competitive adsorption or inhibition on the membrane surfaces. To determine the factors causing a decrease in the H_2 flux with the CO_2 feed, the H_2 flux distribution versus the H_2 fraction of the feed was examined, as shown in Fig. 6.

The H_2 fraction in the feed was proportional to the partial pressure on the feed side. When the partial pressure on the permeate side was constant because of the sweep gas rate being set as a constant, the slope of the line relating the H_2 fraction in the feed and the H_2 flux is a fixed value and follows Sieverts-Fick's law. From Fig. 6, it can be seen that all the experimental points involving CO_2 (see specified points in Runs 4, 5, and 6) were in the region, through which the Sieverts-Fick's line (red-dashed line) passes. The Sieverts-Fick's line also passes through the points in the experiments with a binary feed of H_2 and N_2 (see specified points in Runs 1, 2, and 3). Thus, the effect of CO_2 was similar to that of N_2 on the surface of the Pd82–Ag18/α-Al_2O_3 membrane. The presence of all the test points on the Sieverts-Fick's line indicates that the decrease in the H_2 gain, when the amount of CO_2 in the feed was increasing, was due to dilution (and not inhibition), as is the case with N_2, as discussed in the previous section. Similar results were also reported elsewhere [22,23,36,37,40]. In addition, this result was also consistent with the results of the membrane stability experiments, which did not indicate significant membrane deactivation for more than 7 h of operation. In a feed containing a large CO_2 fraction (Run 5), the H_2 fraction in the feed was so small that the H_2 flux passing through the membrane was negligible; as a result the *HR* was very low.

The presence of a large CO_2 fraction in the feed led to an increasing number of CO_2 molecules residing in the membrane interface layer, thus increasing the external membrane mass transfer resistance. This made it more difficult for H_2 to permeate through the interface layer; therefore, the gradient of the H_2 concentration along the membrane became smaller than it should be. A schematic diagram of the concentration polarization event was reported by Caravella and Sun [29]. A comparison of the effects of N_2 and CO_2 are summarized in Table 5. The effect of these two gases was compared when they had a relatively equal fraction of the feed, which was from Run 1 (representing the effect of N_2) and Run 5 (representing the CO_2 effect). Both these runs were performed under similar conditions with a feed containing a H_2 fraction of approximately 55%.

From Tables 5 and it appears that the average *HR* value, H_2 flux (J_{H2}), partial pressure difference for permeation at each point, as well as the decreasing gradient value of the H_2 concentration along the membrane for Run 5 (H_2/CO_2 feed) were greater than those of Run 1 (H_2/N_2 feed). This is reasonable because Run 5 had a slightly larger fraction of H_2 in the feed than Run 1. A crucial distinction was that the time lag of the two experiments was not identical; the time-lag in Run 5 (larger H_2/CO_2 feed), and its start-up oscillation were greater than those of Run 1 (H_2/N_2 feed). In addition, the reduction in the H_2 concentration fraction along the membrane owing to the concentration polarization for Run 5 was also greater than that of Run 1. However, the H_2 fraction in Run 5 was larger than that in Run 1. This indicates that the CO_2 concentration polarization effect was greater than that of N_2. This is in accordance with Barreiro et al. [36]. The larger size of the CO_2 molecule compared to that of N_2 was responsible for the greater polarization effect of CO_2. The polarization of the concentration in the film layer around the membrane surface manifested as the resistance of the external mass transfer for H_2 to move through the film layer. Relative to time lag, the presence of H_2 permeation barriers in the form of concentration polarization prevented the H_2 adsorption and desorption mechanism from reaching an equilibrium sooner after the start-up. Hence, this process took a longer time.

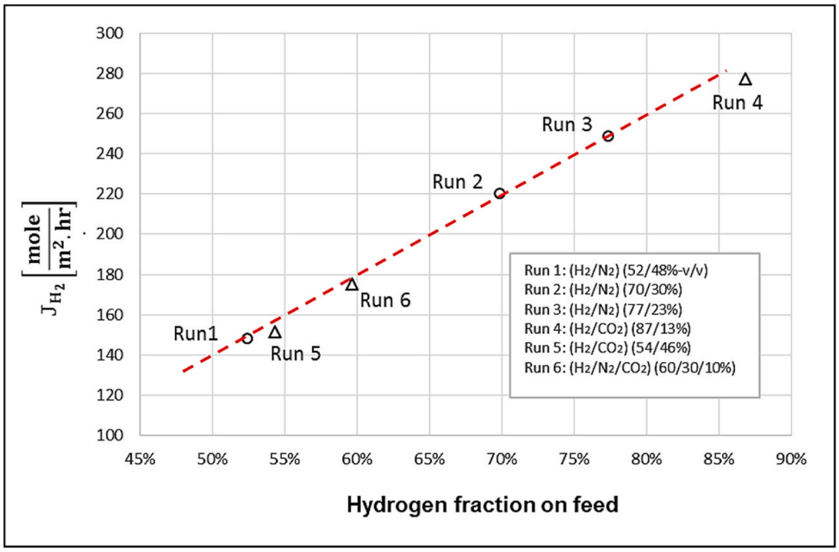

Fig. 6. Graph of hydrogen fraction in feed to hydrogen flux due to CO_2 gas (triangle-shaped point). The white circle displays the experimental results with a H_2/N_2 binary feed. The red dotted line is the Sieverts-Fick's line. (For interpretation of the references to colour in this figure legend, the reader is referred to the Web version of this article.)

Table 5
Comparison of effect of N_2 and CO_2 on Pd82–Ag18/α-Al_2O_3 membrane performance.

	Run 1	Run 5
Condition of feed		
H_2 fraction on feed	52%	54%
N_2 fraction on feed	48%	–
CO_2 fraction on feed	–	46%
Results		
Averaged *HR* (%)	22.0	22.2
J_{H2} (mole/(m^2·h))	148.2	151.5
Partial pressure difference for permeation at each point (kPa)	41.4	42.8
The decreasing gradient of the fractional concentration of hydrogen along the membrane (%mole cm^{-1})	1.23	1.3
Time lag (h)	±2	±3
The reduction of the gradient decreases from the fraction of hydrogen concentration along the membrane as a result of the concentration polarization indication (%mole cm^{-1})	0.8	1.1

3.4. Effect of CO on the performance of the Pd82Ag18/α-Al_2O_3 membrane

The effect of CO on the membrane was observed by introducing (i) a binary mixture of H_2 and CO (80% and 20% v/v, respectively); (ii) a ternary feed, either with the addition of CO_2 or N_2, for example, H_2/CO/CO_2 (68%/19%/13% v/v) and H_2/CO/N_2 (62%/15%/23% v/v); and (iii) a quaternary feed, which was a mixture of H_2/CO/N_2/CO_2 (56%/11%/24%/9% v/v). Fig. 7 (a) shows the stability of *HR* for the binary feed of H_2 and CO, whereas Fig. 7 (b) shows the stability of *HR* for the quaternary feed, (H_2/CO/N_2/CO_2). The *HR* was calculated based on the ratio of the permeated H_2 to the amount of H_2 in the feed. The average *HR* was calculated after its value had a certain inclination (i.e., after the start-up period).

In Fig. 7, it appears that the *HR* fluctuated during the start-up period, after which, it consistently decreased over the duration of the operation. The time-lag of the membrane operation ranged from 3 to 4 h. In the experiments involving CO, the tendency of the membrane deactivation was evident over the operation period of 8 h. The experimental results of the CO concentration variation versus the membrane performance are summarized in Table 6.

Furthermore, Fig. 8 shows a decrease in the H_2 flux at any given time in the binary and quaternary feed experiments. A similar phenomenon was reported by Li et al. [41]. Peters et al. [56] and Caravella et al. [27] suggested that the decrease in the H_2 flux in multi-component feeds was caused by various factors, including dilution and the presence of competitive adsorption or inhibition on the membrane surfaces.

To elaborate the factors causing the decrease in the H_2 flux with a CO feed, the H_2 flux distribution of the H_2 fraction in the feed, is plotted in Fig. 9. This figure is a compilation of all the experiments discussed in the previous section (Runs 1–6). The H_2 fraction in the feed was proportional to the partial pressure on the feed side. When the partial pressure on the permeate side was constant owing to the constant sweep gas rate, the slope of the graph of the hydrogen fraction in the feed versus the H_2 flux was a fixed value and followed Sieverts-Fick's law. Unlike in the previous experiments on N_2 and CO_2 that had experimental points located on the Sieverts-Fick's line, from Fig. 9, it appears that all the observation points of influence of CO on the membrane were below the Sieverts-Fick's line (dashed-red line). This indicates that CO had an inhibitory effect on the surface of the Pd82Ag18/α-Al_2O_3 membrane.

The order of the gaps between the Sieverts-Fick's line and the data plotting points in the CO gas experiment, from the largest to the smallest is as follows: (see the vertical black arrow pointing downward in Fig. 9): Run 7 > Run 8 > Run 9 > Run 10. This is reasonable as Run 7 had the largest CO fraction in the feed (CO fraction in Run 7 > Run 8 > Run 9 > Run 10). Thus, the higher the CO fraction in the feed, the more significant the CO inhibition. Similar results were reported by Barbieri et al. [37], Caravella et al. [27], and Kurokawa et al. [43] At the same time, according to Peters et al. [56], the polarization effect of the concentration and dilution was not significant compared to the effect of CO inhibition on the membrane surfaces. CO significantly inhibited the Pd membrane because the bond between the C atoms in CO and Pd was in the covalent bond range. According to Gallucci et al. [40], the bonds were very close (closer than those for Pd–CO_2 or Pd–N_2, which were influenced by van der Waals forces only). This caused the CO–Pd bonds to be stable, resulting in a significant inhibitory effect on the Pd membrane. A comparison of the bonding distance between CO, CO_2, and N_2 and Pd were reported by Gallucci et al. [40]. Caravella et al. [27] also observed that the effect of CO inhibition was reversible. In addition, to compare the effects of CO and N_2 gases, binary experiments having similar H_2 feed fractions, i.e., Run 3 (representing the effect of N_2) and Run 7 (representing the effect of CO) were compared. Both the experiments had a H_2 feed fraction of approximately 80%. This comparison is presented in Table 7. The HR of the experiments involving CO decreased over time. The H_2 flux in Run 3 (involving N_2) was 248.8 (mole/(m^2·h)), while that in Run 7 (involving CO) decreased from 194.5 to 177.6 (mole/(m^2·h)). Moreover, the H_2 feed fraction in Run 7 was slightly greater than that in Run 3. Over an 8-h operation, the hydrogen flux of Run 7 was approximately 72% of that in Run 3. This indicates that the CO inhibition significantly decreased the H_2 flux.

Furthermore, the effect of temperature in the presence of CO on the feed gas was investigated with conclusion that H_2 permeation reduction is significant at low temperatures [27,41–43]. In this study, another run was conducted with a binary feed of H_2 and CO (80%/20% v/v) at temperatures of 250 and 350 °C. It can be seen that the operation of the Pd82Ag18/α-Al_2O_3 membrane in the same feed, that is binary H_2/CO (80%/20% v/v) at 250 °C decreased the hydrogen flux to 162 mol/(m^2·h), or in other words decreased by 33 mol/(m^2·h) when compared to the operation at 350 °C. The average *HR* also decreased from 26% at 350 °C to 22% for at 250 °C. Li

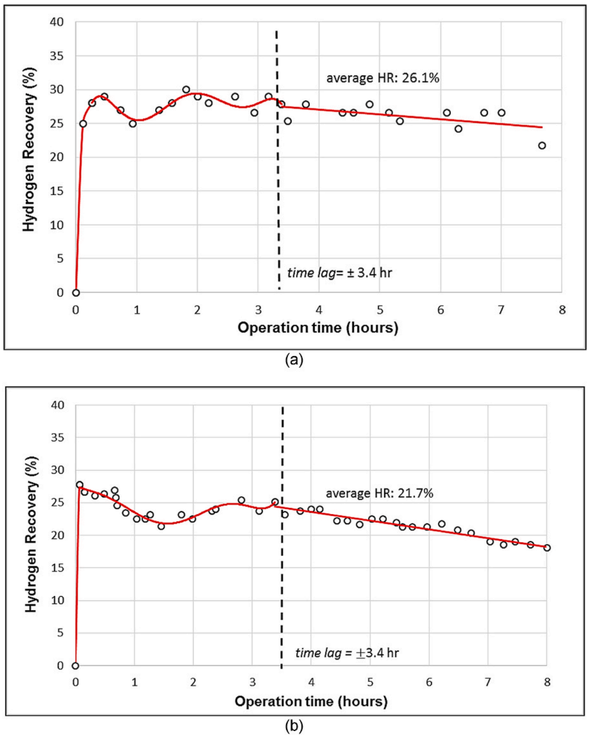

Fig. 7. The stability of hydrogen (*HR*) recovery over the time of membrane operation in the feed gas which is (a) a mixture of H_2/CO gas with an 80/20 mol ratio and (b) a mixture of H_2/CO/N_2/CO_2 with a mole ratio of 56/11/24/9. White spots display HR per unit of experiment time; the red line is the auxiliary line to see the dynamic trend of HR every time; the black vertical dotted line represents the time line where HR has a fixed tendency. (For interpretation of the references to colour in this figure legend, the reader is referred to the Web version of this article.)

Table 6
The result of observation of the influence of CO on the performance of membrane Pd82Ag18/α-Al_2O_3.

	Run 7	Run 8	Run 9	Run 10
H_2 fraction on feed	80%	68%	62%	56%
CO fraction on feed	20%	19%	15%	11%
N_2 fraction on feed	–	–	23%	24%
CO_2 fraction on feed	–	13%	–	9%
Time lag (hours)	±3.4	±3.8	±3.2	±3.4
Averaged HR (%)	26.1	24.4	23.8	21.7
$J_{H2,initial}$ (mole/(m^2.hr))	194.5	186.6	169.6	160.6
$J_{H2\ final}$ (mole/(m^2.hr))	177.6	151.5	161.7	127.8
J_{H2} decline rate throughout operation time (mole/(m^2.hr))/hr	5.0	2.4	9.3	10.5

et al. [41] explained that a decrease in the temperature would make the adsorption of CO on the surface of the membrane stronger. This was reflected in the large value of the CO adsorption constant at low temperatures. More CO adsorbed on the surface of the membrane meant that the more CO covered the adsorption sites for H_2, and consequently, a lower H_2 flux.

4. Conclusions

The H_2 separation from a mixed gas containing N_2, H_2, CO, and CO_2 was performed using a Pd82–Ag18/α-Al_2O_3 membrane. The Pe_{H_2} value on the Pd82–Ag18/α-Al_2O_3 membrane was found to be approximately 3.23×10^{-4} mol m/(m^2·h·kPa$^{0.5}$). In the stability test under a steady state for 8 h, there was no membrane deactivation in the form of decreased *HR* and H_2 flux at any time owing to the presence of N_2 and CO_2 compounds. The decrease in the H_2 flux because of both compounds was due to dilution and concentration polarization. The Pd82Ag18/α-Al_2O_3 membrane had a significantly decreased flux and *HR* owing to CO in the feed gas. The greater the CO concentration and lower the operating temperature, the more significant the inhibition. The higher the co-existing gas fraction in the feed, the lower the H_2 flux. The order of the influence of the co-existing gases in terms of their effect on the H_2 flux was CO > CO_2 > N_2 as can be seen from Sieverts-Fick's line mapping.

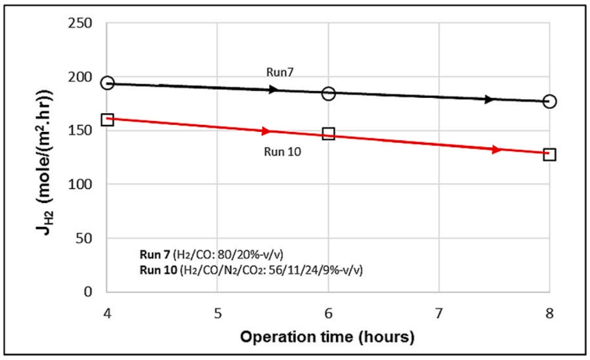

Fig. 8. Hydrogen flux per unit of time in gas mixture gas mixture H_2/CO with mole ratio 80/20 (white circle) and mixture of $H_2/CO/N_2/CO_2$ with mole ratio 56/11/24/9 (white box). The black and red arrows and arrows are the auxiliary lines to see the tendency to decrease the hydrogen flux each time. (For interpretation of the references to colour in this figure legend, the reader is referred to the Web version of this article.)

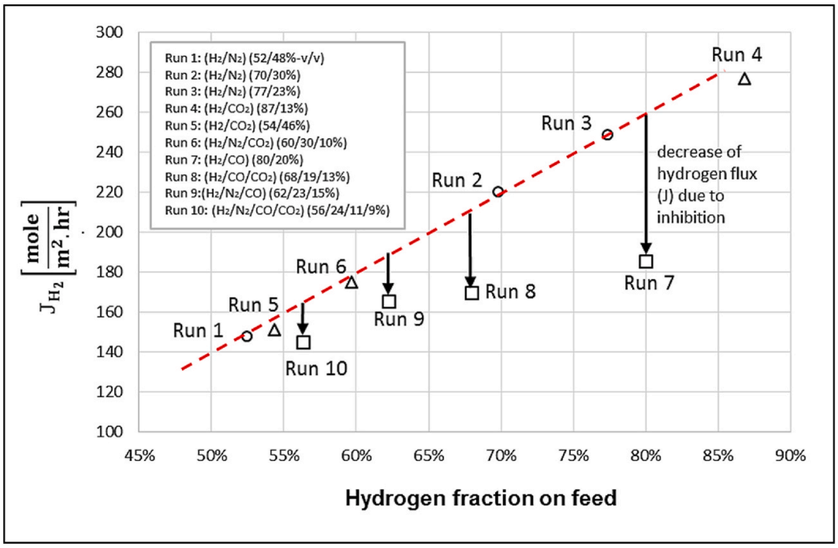

Fig. 9. Graph of hydrogen fraction in feed to hydrogen flux due to CO gas. The red dotted line is the Sieverts-Fick's line. Points labelled numbers 1 through 6 are experimental data with N_2 and CO_2 gases while points labelled 7 to 10 are experimental data of CO gas effect. The black arrow downwards shows the flux reduction of the Sieverts-Fick's line due to inhibition. (For interpretation of the references to colour in this figure legend, the reader is referred to the Web version of this article.)

Table 7
Comparison of effect of N_2 and CO on Pd82Ag18/α-Al_2O_3 membrane performance.

	Run 3	Run 7
H_2 fraction on feed	77%	80%
N_2 fraction on feed	23%	–
CO fraction on feed	–	20%
Whether or not HR declines in 8 h of operation	No	Yes
J_{H2} (mole/(m^2·h))	248.8	194.5 → 177.6
Time lag (h)	±3.0	±3.4

Author contribution statement

Yogi Wibisono Budhi: Conceived and designed the experiments; Analyzed and interpreted the data; Wrote the paper.
Hans Kristian Irawan: Performed the experiments; Analyzed and interpreted the data; Wrote the paper.
Raihan Annisa Fitri, Tareqh Al Syifa Elgi Wibisono, Elvi Restiawaty: Analyzed and interpreted the data; Wrote the paper.
Manabu Miyamoto, Shigeyuki Uemiya: Contributed reagents, materials, analysis tools or data.

Data availability statement

Data included in article/supp. material/referenced in article.

Declaration of competing interest

The authors declare that they have no known competing financial interests or personal relationships that could have appeared to influence the work reported in this paper.

Acknowledgement

The financial support provided by The Indonesia Endowment Fund for Education (LPDP), Indonesian Science Fund (DIPI), and the Ministry of Finance of Indonesia [grant number: RISPRO/KI/BI/KOM/II/16507/I/2020] was gratefully acknowledged. This research is also partially funded by the Indonesian Ministry of Education, Culture, Research, and Technology under World Class Professor 2022.

References

[1] S.M. Jokar, A. Farokhnia, M. Tavakolian, M. Pejman, P. Parvasi, J. Javanmardi, F. Zare, M.C. Gonçalves, A. Basile, The recent areas of applicability of palladium based membrane technologies for hydrogen production from methane and natural gas: a review, Int. J. Hydrogen Energy 48 (2023) 6451–6476, https://doi.org/10.1016/J.IJHYDENE.2022.05.296.
[2] Y. Han, W.S.W. Ho, Recent advances in polymeric facilitated transport membranes for carbon dioxide separation and hydrogen purification, J. Polym. Sci. 58 (2020) 2435–2449, https://doi.org/10.1002/pol.20200187.
[3] W.H. Chen, Z.Y. Chen, S. Lim, Y.K. Park, P.L. Show, Hydrogen permeation in a palladium membrane tube: impacts of outlet and vacuum degree, Int. J. Hydrogen Energy 47 (2022) 40787–40802, https://doi.org/10.1016/J.IJHYDENE.2021.07.182.
[4] J. Xiao, C. Li, L. Fang, P. Böwer, M. Wark, P. Bénard, R. Chahine, Machine learning–based optimization for hydrogen purification performance of layered bed pressure swing adsorption, Int. J. Energy Res. 44 (2020) 4475–4492, https://doi.org/10.1002/er.5225.
[5] K. Sun, T. Yang, S. Ma, F. Ye, J. Xiao, Hydrogen purification performance of pressure swing adsorption based on Cu-BTC/zeolite 5A layered bed, J. Wuhan Univ. Technol.-Materials Sci. Ed. 37 (2022) 815–822, https://doi.org/10.1007/s11595-022-2601-4.
[6] D.-K. Oh, K.-Y. Lee, J.-S. Park, Hydrogen purification from compact palladium membrane module using a low temperature diffusion bonding technology, Membranes 10 (2020), https://doi.org/10.3390/membranes10110338.
[7] K.A.J. Koua, L. Tong, T. Yang, J. Xiao, High purity hydrogen production by metal hydride system: a parametric study based on the lumped parameter model, J. Wuhan Univ. Technol.-Materials Sci. Ed. 36 (2021) 127–135, https://doi.org/10.1007/s11595-021-2385-y.
[8] H. Wang, Y. Liu, J. Zhang, Hydrogen purification by Mg alloy hydrogen adsorbent, Adsorption 28 (2022) 85–95, https://doi.org/10.1007/s10450-021-00348-2.
[9] M. Yang, J. Zhou, L. Gao, The purification of hydrogen isotopes expelled from nuclear fusion reactors by a combined process, Int. J. Hydrogen Energy 45 (2020) 13596–13600, https://doi.org/10.1016/J.IJHYDENE.2018.04.189.
[10] M.M. Barreiro, M. Maroño, J.M. Sánchez, Hydrogen separation studies in a membrane reactor system: influence of feed gas flow rate, temperature and concentration of the feed gases on hydrogen permeation, Appl. Therm. Eng. 74 (2015) 186–193, https://doi.org/10.1016/j.applthermaleng.2013.12.035.
[11] J. Okazaki, D.A.P. Tanaka, M.A.L. Tanco, Y. Wakui, F. Mizukami, T.M. Suzuki, Hydrogen permeability study of the thin Pd–Ag alloy membranes in the temperature range across the α–β phase transition, J. Membr. Sci. 282 (2006) 370–374, https://doi.org/10.1016/j.memsci.2006.05.042.
[12] B. Chantaramolee, A.A.B. Padama, H. Kasai, Y.W. Budhi, First principles study of N and H atoms adsorption and NH formation on Pd(111) and Pd3Ag(111) surfaces, J. Membr. Sci. 474 (2015) 57–63, https://doi.org/10.1016/j.memsci.2014.09.048.
[13] S. Uemiya, T. Matsuda, E. Kikuchi, Hydrogen permeable palladium-silver alloy membrane supported on porous ceramics, J. Membr. Sci. 56 (1991) 315–325, https://doi.org/10.1016/S0376-7388(00)83041-0.
[14] A.A.B. Padama, H. Kasai, Y.W. Budhi, Hydrogen absorption and hydrogen-induced reverse segregation in palladium–silver surface, Int. J. Hydrogen Energy 38 (2013) 14715–14724, https://doi.org/10.1016/j.ijhydene.2013.08.138.
[15] I. Orakwe, H. Shehu, E. Gobina, Preparation and characterization of palladium ceramic alumina membrane for hydrogen permeation, Int. J. Hydrogen Energy 44 (2019) 9914–9921, https://doi.org/10.1016/j.ijhydene.2019.01.033.
[16] S. Smart, S. Liu, J.M. Serra, J.C. Diniz da Costa, A. Iulianelli, A. Basile, 8 - porous ceramic membranes for membrane reactors, in: A.B. T.-H, M.R. Basile (Eds.), Woodhead Publishing Series in Energy, Woodhead Publishing, 2013, pp. 298–336, https://doi.org/10.1533/9780857097330.2.298.
[17] D. Alique, M. Imperatore, R. Sanz, J.A. Calles, M. Giacinti Baschetti, Hydrogen permeation in composite Pd-membranes prepared by conventional electroless plating and electroless pore-plating alternatives over ceramic and metallic supports, Int. J. Hydrogen Energy 41 (2016) 19430–19438, https://doi.org/10.1016/j.ijhydene.2016.06.128.
[18] X. Tan, K. Li, 7 - dense ceramic membranes for membrane reactors, in: A.B. T.-H, M.R. Basile (Eds.), Woodhead Publishing Series in Energy, Woodhead Publishing, 2013, pp. 271–297, https://doi.org/10.1533/9780857097330.2.271.
[19] J.M. Vásquez Castillo, T. Sato, N. Itoh, Effect of temperature and pressure on hydrogen production from steam reforming of biogas with Pd–Ag membrane reactor, Int. J. Hydrogen Energy 40 (2015) 3582–3591, https://doi.org/10.1016/j.ijhydene.2014.11.053.
[20] H.M. Faizal, R. Kizu, Y. Kawamura, T. Yokomori, T. Ueda, Effect of feed flow rate of hydrogen mixture on hydrogen permeation for flat sheet Pd/Ag membrane with stagnating flow, J. Therm. Sci. Technol. 8 (2013) 120–135, https://doi.org/10.1299/jtst.8.120.
[21] C. Brencio, F.W.A. Fontein, J.A. Medrano, L. Di Felice, A. Arratibel, F. Gallucci, Pd-based membranes performance under hydrocarbon exposure for propane dehydrogenation processes: experimental and modeling, Int. J. Hydrogen Energy 47 (2022) 11369–11384, https://doi.org/10.1016/J.IJHYDENE.2021.09.252.
[22] K. Hou, R. Hughes, The effect of external mass transfer, competitive adsorption and coking on hydrogen permeation through thin Pd/Ag membranes, J. Membr. Sci. 206 (2002) 119–130, https://doi.org/10.1016/S0376-7388(01)00770-0.
[23] J. Boon, J.A.Z. Pieterse, F.P.F. van Berkel, Y.C. van Delft, M. van Sint Annaland, Hydrogen permeation through palladium membranes and inhibition by carbon monoxide, carbon dioxide, and steam, J. Membr. Sci. 496 (2015) 344–358, https://doi.org/10.1016/j.memsci.2015.08.061.
[24] Y. Sakamoto, F.L. Chen, Y. Kinari, F. Sakamoto, Effect of carbon monoxide on hydrogen permeation in some palladium-based alloy membranes, Int. J. Hydrogen Energy 21 (1996) 1017–1024, https://doi.org/10.1016/S0360-3199(96)00069-9.
[25] H. Li, A. Goldbach, W. Li, H. Xu, CO2 decomposition over Pd membrane surfaces, J. Phys. Chem. B 112 (2008) 12182–12184, https://doi.org/10.1021/jp806587y.
[26] W. Wang, X. Pan, X. Zhang, W. Yang, G. Xiong, The effect of co-existing nitrogen on hydrogen permeation through thin Pd composite membranes, Sep. Purif. Technol. 54 (2007) 262–271, https://doi.org/10.1016/j.seppur.2006.09.016.
[27] A. Caravella, F. Scura, G. Barbieri, E. Drioli, Inhibition by CO and polarization in Pd-based membranes: a novel permeation reduction coefficient, J. Phys. Chem. B 114 (2010) 12264–12276, https://doi.org/10.1021/jp104767q.
[28] A. Brunetti, A. Caravella, E. Fernandez, D.A. Pacheco Tanaka, F. Gallucci, E. Drioli, E. Curcio, J.L. Viviente, G. Barbieri, Syngas upgrading in a membrane reactor with thin Pd-alloy supported membrane, Int. J. Hydrogen Energy 40 (2015) 10883–10893, https://doi.org/10.1016/j.ijhydene.2015.07.002.

[29] A. Caravella, Y. Sun, Correct evaluation of the effective concentration polarization influence in membrane-assisted devices. Case study: H2 production by Water Gas Shift in Pd-membrane reactors, Int. J. Hydrogen Energy 41 (2016) 11653–11659, https://doi.org/10.1016/j.ijhydene.2015.12.068.
[30] Y.W. Budhi, I. Noezar, F. Aldiansyah, P.V. Kemala, A.A.B. Padama, H. Kasai, Subagjo, Forced unsteady state operation to improve H2 permeability through Pd–Ag membrane during start-up, Int. J. Hydrogen Energy 36 (2011) 15372–15381, https://doi.org/10.1016/j.ijhydene.2011.08.110.
[31] Y.W. Budhi, H. Rionaldo, A.A.B. Padama, H. Kasai, I. Noezar, Forced unsteady state operation for hydrogen separation through Pd–Ag membrane after start-up, Int. J. Hydrogen Energy 40 (2015) 10081–10089, https://doi.org/10.1016/j.ijhydene.2015.05.182.
[32] Y.W. Budhi, W. Suganda, H.K. Irawan, E. Restiawaty, M. Miyamoto, S. Uemiya, N. Nishiyama, M. van Sint Annaland, Hydrogen separation from mixed gas (H2, N2) using Pd/Al2O3 membrane under forced unsteady state operations, Int. J. Hydrogen Energy 45 (2020), https://doi.org/10.1016/j.ijhydene.2020.01.235.
[33] P. Pérez, C.A. Cornaglia, A. Mendes, L.M. Madeira, S. Tosti, Surface effects and CO/CO2 influence in the H2 permeation through a Pd–Ag membrane: a comprehensive model, Int. J. Hydrogen Energy 40 (2015) 6566–6572, https://doi.org/10.1016/j.ijhydene.2015.03.106.
[34] Y.W. Budhi, D.D. Putri, A. Husna, H.K. Irawan, M. Miyamoto, S. Uemiya, Dynamic operation of water gas shift reaction over Fe2O3/Cr2O3/CuO catalyst in Pd/Al2O3 membrane reactor, IOP Conf. Ser. Earth Environ. Sci. (2018), https://doi.org/10.1088/1755-1315/105/1/012020.
[35] Y. Bi, H. Xu, W. Li, A. Goldbach, Water–gas shift reaction in a Pd membrane reactor over Pt/Ce0.6Zr0.4O2 catalyst, Int. J. Hydrogen Energy 34 (2009) 2965–2971, https://doi.org/10.1016/j.ijhydene.2009.01.046.
[36] M.M. Barreiro, M. Maroño, J.M. Sánchez, Hydrogen permeation through a Pd-based membrane and RWGS conversion in H2/CO2, H2/N2/CO2 and H2/H2O/CO2 mixtures, Int. J. Hydrogen Energy 39 (2014) 4710–4716, https://doi.org/10.1016/j.ijhydene.2013.11.089.
[37] G. Barbieri, F. Scura, F. Lentini, G. De Luca, E. Drioli, A novel model equation for the permeation of hydrogen in mixture with carbon monoxide through Pd–Ag membranes, Sep. Purif. Technol. 61 (2008) 217–224, https://doi.org/10.1016/j.seppur.2007.10.010.
[38] S.H. Israni, B.K.R. Nair, M.P. Harold, Hydrogen generation and purification in a composite Pd hollow fiber membrane reactor: experiments and modeling, Catal. Today 139 (2009) 299–311, https://doi.org/10.1016/j.cattod.2008.02.020.
[39] S.H. Israni, M.P. Harold, Methanol steam reforming in Pd−Ag membrane reactors: effects of reaction system species on transmembrane hydrogen flux, Ind. Eng. Chem. Res. 49 (2010) 10242–10250, https://doi.org/10.1021/ie1005178.
[40] F. Galluci, F. Chiaravalloti, S. Tosti, E. Drioli, A. Basile, The effect of mixture gas on hydrogen permeation through a palladium membrane: experimental study and theoretical approach, Int. J. Hydrogen Energy 32 (2007) 1837.
[41] H. Li, A. Goldbach, W. Li, H. Xu, PdC formation in ultra-thin Pd membranes during separation of H2/CO mixtures, J. Membr. Sci. 299 (2007) 130–137, https://doi.org/10.1016/J.MEMSCI.2007.04.034.
[42] A.L. Mejdell, M. Jondahl, T.A. Peters, R. Bredesen, H.J. Venvik, Effects of CO and CO2 on hydrogen permeation through a ~3 micron Pd/Ag 23 wt% membrane employed in a microchannel membrane configuration, Sep. Purif. Technol. 68 (2009) 178.
[43] H. Kurokawa, H. Yakabe, I. Yasuda, T. Peters, R. Bredesen, Inhibition effect of CO on hydrogen permeability of Pd–Ag membrane applied in a microchannel module configuration, Int. J. Hydrogen Energy 39 (2014) 17201–17209, https://doi.org/10.1016/j.ijhydene.2014.08.056.
[44] A. Unemoto, A. Kaimai, T. Otake, K. Yashiro, T. Kawada, J. Mizusaki, T. Tsuneki, I. Yasuda, Hydrogen permeability of palladium alloy membrane at high temperatures in the impurity gases co-existing atmospheres, 16th World Hydrogen Energy Conference 2006, WHEC 2006 4 (2006) 3113–3121.
[45] N.R. Roshan, S V Gorbunov, E.M. Chistov, F.R. Karelin, K.A. Kuterbekov, K.Zh Bekmyrza, E.T. Abseitov, Membranes of palladium alloys for ultrapure hydrogen production, Inorg. Mater.: Appl. Res. 11 (2020) 1214–1221, https://doi.org/10.1134/S2075113320050287.
[46] A. Caravella, G. Barbieri, E. Drioli, Modelling and simulation of hydrogen permeation through supported Pd-alloy membranes with a multicomponent approach, Chem. Eng. Sci. 63 (2008) 2149–2160, https://doi.org/10.1016/j.ces.2008.01.009.
[47] S. Uemiya, Y. Kude, K. Sugino, N. Sato, T. Matsuda, E. Kikuchi, A palladium/porous-glass composite membrane for hydrogen separation, Chem. Lett. 17 (1988) 1687–1690, https://doi.org/10.1246/cl.1988.1687.
[48] M. Miyamoto, R. Hayakawa, Y. Makino, Y. Oumi, S. Uemiya, M. Asanuma, CO2 methanation combined with NH3 decomposition by in situ H2 separation using a Pd membrane reactor, Int. J. Hydrogen Energy 39 (2014) 10154–10160, https://doi.org/10.1016/j.ijhydene.2014.04.170.
[49] M. Miyamoto, R. Hayakawa, Y. Makino, Y. Oumi, S. Uemiya, M. Asanuma, CO2 methanation combined with NH3 decomposition by in situ H2 separation using a Pd membrane reactor, Int. J. Hydrogen Energy 39 (2014) 10154–10160, https://doi.org/10.1016/J.IJHYDENE.2014.04.170.
[50] A. Basile, J. Tong, P. Millet, 2 - inorganic membrane reactors for hydrogen production: an overview with particular emphasis on dense metallic membrane materials, in: A.B. T.-H, M.R. Basile (Eds.), Woodhead Publishing Series in Energy, Woodhead Publishing, 2013, pp. 42–148, https://doi.org/10.1533/9780857097330.1.42.
[51] N. Itoh, W.-C. Xu, Selective hydrogenation of phenol to cyclohexanone using palladium-based membranes as catalysts, Appl. Catal. Gen. 107 (1993) 83–100, https://doi.org/10.1016/0926-860X(93)85117-8.
[52] W.-H. Chen, I.-H. Chiu, Transient dynamic of hydrogen permeation through a palladium membrane, Int. J. Hydrogen Energy 34 (2009) 2440–2448, https://doi.org/10.1016/j.ijhydene.2008.12.062.
[53] A. Basile, F. Gallucci, , S.B.T.-M.S., T. Tosti, Synthesis, characterization, and applications of palladium membranes, in: Inorganic Membranes: Synthesis, Characterization and Applications, Elsevier, 2008, pp. 255–323, https://doi.org/10.1016/S0927-5193(07)13008-4.
[54] D. Pizzi, R. Worth, M. Giacinti Baschetti, G.C. Sarti, K. Noda, Hydrogen permeability of 2.5μm palladium–silver membranes deposited on ceramic supports, J. Membr. Sci. 325 (2008) 446–453, https://doi.org/10.1016/j.memsci.2008.08.020.
[55] M. De Falco, L. Marrelli, G. Iaquaniello, Membrane Reactors for Hydrogen Production Process, Springer-Verlag London, 2011, https://doi.org/10.1007/978-0-85729-151-6.
[56] T.A. Peters, M. Stange, H. Klette, R. Bredesen, High pressure performance of thin Pd–23%Ag/stainless steel composite membranes in water gas shift gas mixtures; influence of dilution, mass transfer and surface effects on the hydrogen flux, J. Membr. Sci. 316 (2008) 119–127, https://doi.org/10.1016/J.MEMSCI.2007.08.056.